Solid Earth Discuss., 3, 963–974, 2011
www.solid-earth-discuss.net/3/963/2011/
doi:10.5194/sed-3-963-2011

Solid Earth Discussions

DInSAR coseismic deformation of the May 2011 M_w 5.1 Lorca earthquake, (Southern Spain)

T. Frontera[1], A. Concha[2], P. Blanco[3], A. Echeverria[4], X. Goula[1], R. Arbiol[3], G. Khazaradze[4], F. Pérez[3], and E. Suriñach[4]

[1]Institut Geològic de Catalunya, Seismology Dept., Balmes 209–211, Barcelona 08006, Spain
[2]Institut Geològic de Catalunya, Geological Engineering and Hazards Dept., Balmes 209–211, Barcelona 08006, Spain
[3]Institut Cartogràfic de Catalunya, Remote Sensing Dept., Parc de Montjuïc s/n, Barcelona 08038, Spain
[4]Universitat de Barcelona, Geodynamics and Geophysics Dept., Martí i Franquès s/n, Barcelona 08028, Spain

Received: 14 October 2011 – Accepted: 24 October 2011 – Published: 9 November 2011

Correspondence to: T. Frontera (tfrontera@igc.cat)

Published by Copernicus Publications on behalf of the European Geosciences Union.

Abstract

The coseismic superficial deformation at the region of Lorca (Murcia, southeastern Spain) due to the M_w 5.1 earthquake occurred on 11 May 2011 was studied by a multidisciplinary team, integrating information from DInSAR, GPS and numerical modeling techniques. Despite the moderate magnitude of the event, quantitative information was obtained from the interferometric study of a pair of SAR images. Coseismic vertical deformation was differentiated from subsidence related to groundwater extraction at the footwall block through a numerical modeling deformation estimation based on elastic rupture dislocations. On the other hand, horizontal crustal deformation rates obtained from the analysis of a GPS network existent in the area are also coherent with the mechanism calculated for the earthquake.

1 Introduction

On 11 May 2011, two shallow moderate magnitude earthquakes occurred at less than 5 km northeast of the city of Lorca (Murcia, southeastern Spain). The first event (M_w 4.5) took place at 15:05 (UTC), and had a maximum intensity of VI in the European Macroseismic Scale (EMS). The second and main event (M_w 5.1) occurred at 16:47 (UTC), with an epicenter of coordinates 37.69° N, 1.67° W and a depth of 2 km (IGN, 2011), as shown in Fig. 1. This main event, which was assigned a maximum intensity of VII (IGN, 2011), caused extensive damages to dwelling buildings, schools and monuments (Irizarry et al., 2011), but did not cause surface rupture. The earthquakes took place at the eastern part of the Betic Cordillera, along the Alhama de Murcia fault (FAM) (Bousquet, 1979). It is a highly seismogenic oblique slip (reverse-sinister) fault; with a strike between N45° E and N65° E; a maximum slip rate of 0.3 mm yr^{-1}, measured in recent trenches, and located close to the convergent plate limit between Eurasian and African plates, with a total regional rate of 4–5 mm yr^{-1} (Masana et al., 2004). The convergence direction of this fault has remained constant since late Miocene to nowadays (Martínez-Díaz, 2002).

SED
3, 963–974, 2011

The Lorca main event focal mechanism (M_w 5.1) (Delouis, 2011) shows a reverse sinister motion, compatible with geological and GPS observations. One of the calculated fault planes coincides with the same orientation of the FAM (Fig. 1).

The aftershock events decrease quickly through time to less than five events per day in five days. Curiously, these events are not located along the inferred FAM fault plane, dipping towards NNW, but rather they are spread in seemingly non-linear fashion towards the SE from the main shock into the Alto Guadalentín Valley (AGV). This supposed misallocation might be due to the generation of aftershocks in a zone with a high concentration of the static Mohr-Coulomb stress out of the FAM plane (IGN,2011).

2 GPS data

The CuaTeNeo (Cuantificiación de la Tectónica actual y Neotectónica) geodetic network consists of 15 points, specifically built in 1996 to quantify the current rates of crustal deformation in the eastern part of the Betic Cordillera (Colomina et al., 1999).

Horizontal velocities at stations on the SE side of the FAM (PURI and GANU) show oblique compression with left-lateral direction of motion of $1.9 \pm 0.5\,\mathrm{mm\,yr^{-1}}$ relative to the stations on the NW (MELL and TERC) in accordance to geological observations and focal mechanism of the Lorca earthquake (Fig. 1). The GPS velocities are based on observations of the campaigns performed in 1997, 2002, 2006 (e.g. Khazaradze et al., 2008) and 2009.

Shortly after the occurrence of the earthquake, a new GPS measurement of the nearby CuaTeNeo sites was performed. However, the preliminary results do not show any detectable co-seismic deformation at the sites, mainly due to their remoteness from the main event epicenter. Nevertheless, the analysis of the continuous GPS site LORC, belonging to the Meristemum network (Garrido et al., 2011) and located within the city of Lorca (Fig. 1), shows a co-seismic jump of about 5 mm towards the north in the N-S component on the day of the Lorca earthquake, with no detectable displacements in E-W direction. It must be pointed out that this site presented a very anomalous

SED
3, 963–974, 2011

long-term motion with prominent subsidence of $98.5 \pm 1.9\,\mathrm{mm\,yr^{-1}}$ (Table 1) since 2008 and before the earthquake (Echeverria et al., 2011).

3 DInSAR images

The use of Synthetic Aperture Radar Differential Interferometry (DInSAR) technique for quantifying coseismic deformations has been previously used at the Africa-Eurasian plate boundary at the western Mediterranean area, e.g. in Morocco (Belabbes et al., 2009; Akoglu et al., 2006); and in the Iberian Peninsula, also at the same seismogenic area in the Betic Cordillera (González et al., 2009). Nevertheless, this is the first time in this area that a processing has been performed immediately after the occurrence of a seismic event and it has been compared to theoretical numerical modeled vertical elastic deformation based on estimated seismic rupture dislocation.

A DInSAR processing (Hanssen, 2001; Mora et al., 2007) of one pre- and one post-event stripmap TerraSAR-X image (25 July 2008 and 14 May 2011) was performed for the Lorca event. In order to reduce temporal decorrelation and avoid non-seismic deformation phenomena, a shorter temporal baseline would be desirable. Unfortunately, that was the only pre-event image available in the TerraSAR-X archive for the study zone. Topography was cancelled employing an interpolated SRTM DTM. Atmospheric effects were considered nonsignificant as the detected fringe spatial gradient does not correspond to the typical atmospheric one (Hanssen, 2001).

Figure 2a shows the filtered deformation fringes of the differential phase in radians. Each color cycle is equivalent to a deformation of 1.55 cm along the line of sight of the radar (~35° of incidence angle). The well marked fringe pattern is aligned along the trace of the FAM, showing a defined deformation gradient perpendicular to its trace. Further to the S and SE of the epicentral area, the quality of the signal (measured by the coherence parameter) is lower outside the urban areas, mostly associated to agricultural fields in the AGV, and showing a concentric low coherence fringe pattern.

SED
3, 963–974, 2011

A vertical displacement map was generated by unwrapping the phase of the differential interferogram (Costantini, 1998). A high coherence pixel with a zero deformation value according to the numerical model (see next section) was employed to fix the solution. A median filter was applied to the deformation map to reduce the impact of the low coherence pixels (Fig. 2b).

The northern (hangingwall) block of the fault has a maximum upward movement of about 3 cm that agrees with the reported focal mechanism, while the southern (footwall) block of the fault shows a maximum downward movement of 18 cm. There is a remarkable difference of order of magnitude between the displacements in each one of the blocks. The limit of these movement tendencies coincides clearly with the FAM trace (Fig. 2a), reflecting also the local change in the strike of the fault from N35° E to N60° E and the geological contrasts between the sediments of AGV and the Tertiary rocks of Sierra de la Tercia (TS).

The downward movement of 18 cm in the southern block (Fig. 2b) would represent a constant rate of movement of about 64.2 mm yr^{-1}, which would be comparable to the LORC GPS measurements, reported in the previous section (Table 1).

4 Numerical model of coseismic vertical deformation

The vertical superficial deformation numerical model produced by the Mw 5.1 earthquake was generated using the method of Wang et al. (2003), which considers an elastic deformation field. In a first step, the Green's functions are computed for a number of source depths and distances, depending on the given layered half-space velocity crustal model. In this case, the chosen crustal model was taken from Dañobeitia et al. (1998) that consists of 7 layers between 0 and 35 km in depth.

A rectangular rupture surface was chosen and defined by six fault parameters: slip, length, width, strike, dip and rake of the dislocation. For the present work, the first three parameters were set at 15 cm, 4 km and 2 km respectively, attending to the mean values for this magnitude range given by Wells and Coppersmith (1994) and in agreement

SED
3, 963–974, 2011

with the seismic moment (4.9×10^{23} dyn cm) in accordance with the M_w 5.1 given by Delouis (2011), whose moment tensor inversion has been used to determine the orientation and dislocation of the fault, i.e., 245° for the strike, 65° for the dip and 58° for the rake. According to the hypocenter depth of 2 km, and a fault width of 2 km, we assume that the top of the rupture stops at a depth of 1 km (Fig. 2b).

The maximum predicted vertical deformations are up to 1 cm downwards 2 km to the SE and around 4 cm upwards 2 km to the NW from the epicenter (Fig. 2b). As shown in Table 1, even if there is a good agreement between DInSAR and numerical model results in the northern block, there is a noticeable discrepancy in the southern block.

5 Discussion and conclusions

Using the numerical model as reference for the coseismic displacement, we found a good agreement between the DInSAR measurements (3 cm) and the model estimated values (4 cm) on the northern hangingwall block of the fault. This match, as well as the distribution of the vertical movement gradient along the FAM trace, allows to state that the numerical model is a good approximation of the coseismic deformation (Fig. 2b). The largest difference is the areal extent of the deformation and concentration of displacements on the northwestern sector of the study area. This difference might be due to changes of geology and definition of local tectonic blocks (Martínez-Díaz, 2002) in the area, and to a possible heterogeneous rupture process, not considered in our uniform dislocation model.

On the other hand, there are noteworthy disagreements related to the southern block both with DInSAR and GPS (LORC station) results (Table 1). González and Fernández (2011) report important subsidence rates (Table 1) at the AGV sedimentary basin, of about 100 mm yr^{-1}, due to intensive groundwater extraction, which could be responsible of the large differences obtained by numerical and field techniques (DInSAR and GPS).

SED
3, 963–974, 2011

This intensive groundwater extraction might generate changes of the stress field that could explain the location of the aftershocks (IGN, 2011) out of the FAM trace, but further away within AGV (Fig. 1).

While the predicted coseismic deformation is of the order of few centimeters, subsidence related deformation is of the order of tens of centimeters. Comparisons between results obtained from different techniques for the southern block, as well as the DInSAR differences between northern and southern blocks, allow differentiating coseismic deformation from the groundwater extraction related subsidence accumulated between 2008 and 2011.

By combining remote sensing measurements (DInSAR), in-situ field measurements (CuaTeNeo GPS network) and numerical models of fault rupture, we were able to characterize the coseismic deformation for the 11 May 2011, M_w 5.1 earthquake. Horizontal crustal deformation rates and directions obtained from preexisting GPS data are coherent with the mechanism calculated for the earthquake. The main differences were obtained in the vertical component movement. Complementing the numerical results with the other two techniques, permitted the differentiation of the coseismic movement from those locally affecting the city of Lorca and AGV, since large water extraction-related subsidence highly alters the strain-stress state on the southern block of the FAM.

This is the first time that results from interferometry technique are obtained and confirmed by a multi-technique and multi-disciplinary study for an earthquake in Spain.

Acknowledgements. The authors would like to thank INFOTERRA for providing the TerraSAR-X images and the Instituto Geológico Minero Español (IGME) for providing helpful information of the area; the Spanish Ministerio de Ciencia e Innovación project CuaTeNeo (CGL2004-21666-E); the University of Barcelona (UB) APIF pre-doctoral grant to A. E; Financial support by the UB Faculty of Geology and the Laboratori d'Estudis Geofísics Eduard Fontserè of Institut d'Estudis Catalans. We thank the numerous volunteers, who have participated in the field campaigns.

SED
3, 963–974, 2011

References

Akoglu, A. M., Cakir, Z., Meghraoui, M., Belabbes, S., El Alami, S. O., Ergintav, S., and Akyuz, H. S.: The 1994–2004 Al Hoceima (Morocco) earthquake sequence: Conjugate fault ruptures deduced from InSAR, Earth Planet. Sci. Lett., 252, 467–480, 2006.

Belabbes, S., Wicks, C., Cakir, Z., and Meghraoui, M.: Rupture parameters of the 2003 Zemmouri (Mw 6.8), Algeria, earthquake from joint inversion of interferometric synthetic aperture radar, coastal uplift, and GPS. J. Geophys. Res.-Sol. Ea., 11, B03406, doi:10.1029/2008JB005912, 2009.

Bousquet, J. C.: Quaternary strike-slip faults in southeastern Spain, Tectonophysics, 52, 277–286, 1979.

Colomina, I., Fleta, J., Giménez, J., Goula, X., Masana, E., Ortiz, M. A., Santanach, P., Soro, M., Suriñach, E., Talaya, J., and Térmens, A.: The CuaTeNeo GPS network to quantify horizontal movements in the Southeastern of the IberianPeninsula, edited by: Garcia, J. M. and Romacho, M. D., International Symposium Assesment and reduction of natural risk, I Ass. Hispano Portuguesa, Almeria. IGN, SIM1_01.do, 1999.

Costantini, M.: A novel phase unwrapping method based on network programming, IEEE Trans. Geosci. Remote Sens., 36, 813–821, 1998.

Dañobeitia, J. J., Sallarès, V., and Gallart, J.: Local earthquakes seismic tomography in the Betic Cordillera (southern Spain), Earth and Planet. Sci. Lett., 160, 225–239, 1998.

Delouis, B.:http://www.emsc-csem.org/Files/event/221132/result_Lorca_EQ.jpg, 2011.

Echeverria, A., Khazaradze, G., Gárate, J., Asensio, A., Masana, E., and Suriñach, E.: Present-day GPS crustal deformation rates in the Eastern Betics (SE Spain), Geophys. Res. Abstr., 13(EGU2011-8005), 1, 2011.

Garrido, M. S., Gimènez, E., de Lacy, M. C., and Gil, A. J.: Surveying at the limits of local RTK networks: Test results from the perspective of high accuracy users, Int. J. Appl. Earth Obs., 13, 256–264, 2011.

González, P. J., Fernández, J., and Luzón, F.: Interferometría radar aplicada a terremotos de magnitud moderada en las Cordilleras Béticas, SO España (in Spanish), Revista de cartografía, sistemas de información geográfica y teledetección, 133, 18–23,2009.

González P. J. and Fernández, J.: Drougth-driven transient aquifer compaction imaged using multitemporal satellinte radar interferometry, Geology, 39, 551–554, 2011.

Hanssen, R.: Radar Interferometry, Kluwer Academic Publishers, 2001.

SED
3, 963–974, 2011

IGN: Serie terremoto NE Lorca, 11 mayo 2011, http://www.ign.es/ign/resources/sismologia/Lorca.pdf, 2011.

Irizarry, J., Frontera, T., Goula, X., and Barbat, A. H.: Learning from Earthquakes Lorca, Spain, Earthquakes of May 11, 2011, EERI Newsletter, June 2011, 45, 3, 2011.

Khazaradze, G., Gárate, J., Suriñach, E., Dávila, J. M., and Asensio, E.: Crustal deformation in south-eastern Betics from CuaTeNeo GPS network, GeoTemas, 10, 10123–10127, 2008.

Martínez-Díaz, J. J.: Stress field variety related to fault interaction in a reverse oblique-slip fault: the Alhama de Murcia Fault, Betic Cordillera, Spain, Tectonophysics, 356, 291–305, 2002.

Masana, E., Martínez-Díaz, J. J., Hernández-Enrile, J. L., and Santanach, P.: The Alhama de Murcia fault (SE Spain), a seismogenic fault in a diffuse plate boundary: Seismotectonic implications for the Ibero-Magrebian region, J. Geophys. Res., 109, B01301, doi:10.1029/2002JB002359, 2004.

Mora, O., Arbiol, R., and Palà, V.: ICC's Project for DInSAR Terrain Subsidence Monitoring of the Catalonian Territory, Proceedings of IGARSS 2007, 4953–4956, 2007.

Wang, R., Lorenzo-Martín, F., and Roth, F.: Computation of deformation induced by earthquakes in a multi-layered elastic crust – FORTRAN programs EDGRN/EDCMP, Comput. Geosci., 29, 195–207, 2003.

Wells, D. L. and Coppersmith, K. J.: New empirical relationships among magnitude, rupture length, rupture width, rupture area, and surface displacement, Bull, Seismol. Soc. Am. , 84, 974–1002, 1994.

SED

3, 963–974, 2011

Table 1. Comparison of the numerical model vertical displacement results with reported values of maximum displacements and calculated rates from different GPS and DInSAR studies, at both FAM blocks. Negative sign means subsidence.

Technique	Northern block maximum vertical displacement (mm)	Southern block maximum vertical displacement (mm)	Southern block vertical displacement rate (mm yr^{-1})
GPS LORC (2008–2011) (Echeverria et al., 2011)	–	–	−98.5*
DInSAR (2008–2011) (this study)	+30	−180	−64.2
DInSAR (1992–2011) (González and Fernández, 2011)	–	–	−100*
Numerical model Lorca event (this study)	+40	−10	–

* Measurements made before the Lorca earthquake on 11 May 2011.

SED
3, 963–974, 2011

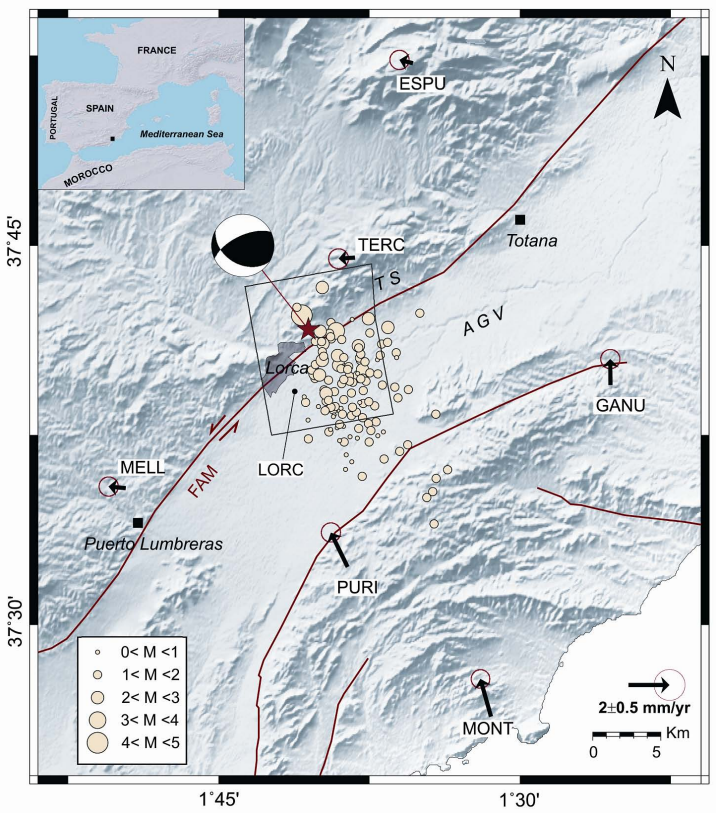

Fig. 1. Study area in SE of Spain, showing the main fault traces in red lines; the GPS stations with their associated horizontal displacement vectors; the epicentral location of the main seismic event (red star) and aftershocks (yellow spots); focal mechanism of the main earthquake. The black contour delimits the area for Fig. 2a and b. AGV: Alto Guadalentín Valley; FAM: Alhama de Murcia Fault; TS: Sierra de la Tercia.

SED
3, 963–974, 2011

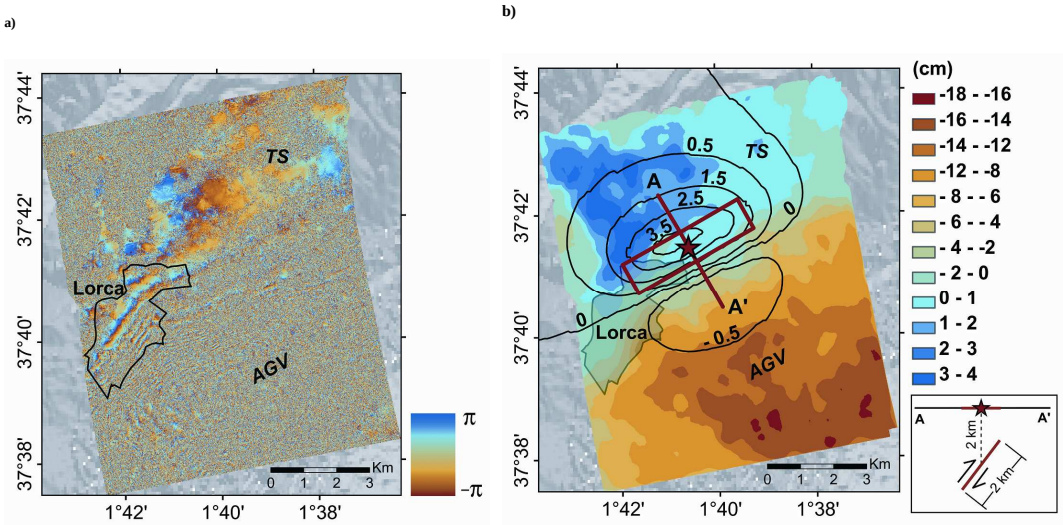

Fig. 2. **(a)** Filtered deformation fringes of the differential interferometric phase in radians. Each colour cycle is equivalent to deformation along the line of sight of about 1.55 cm. The limit of the Lorca urban area is shown for reference; **(b)** Vertical displacement map. The color scale shows the displacement measured by DInSAR. The black curves show the isovalues obtained by the numerical model in cm. The red rectangle and cross-section line show the dimensions and location of the rupture plane considered in the numerical model. The limit of the Lorca urban area is shown for reference.

SED
3, 963–974, 2011